

Effects of surface topography on low Reynolds number droplet/bubble flow through constricted passage

Aditya Singla, and Bahni Ray

Department of Mechanical Engineering, Indian Institute of Technology Delhi

New Delhi - 110016, India

Abstract

This paper is an attempt to study the effects of surface topography on the flow of a droplet (or a bubble) in a low Reynolds number flow regime. Multiphase flows through a constricted passage find many interesting applications in chemistry and biology. The main parameters which determine the flow properties such as flow rate and pressure drop, and govern the complex multiphase phenomena such as drop coalescence, break-up and snap-off in a straight channel flow are the viscosity ratio, droplet size and ratio of the viscous forces to the surface tension forces (denoted by Capillary number). But in flow through a constricted passage, various other parameters such as constriction ratio, length and shape of the constriction, phase angle, and spacing between the constrictions also start playing an important role. An attempt has been made to review and summarize the present knowledge on these aspects and by mentioning what all lacks in the literature that could be studied further.

1. Introduction

Flow of emulsions through porous media finds many useful applications in oil and gas, food, chemical, pharmaceutical, and textile industries [1-8]. To simplify the problem of emulsion flow through porous media, many researchers have treated this problem analogous to drop/bubble flow in a constricted channel. Multiphase flows through a constriction also find use in many biological applications such as detection of cancer cells in the blood [9] and study of mechanical properties of red blood cells and three-dimensional protein networks in the blood [10]. These applications discussed above usually involve low Reynolds number (the ratio of inertial forces to the viscous forces) flows and hence the inertial effects are not so dominant, and various surface and capillary effects start coming into picture.

A very interesting and important field that has recently developed with low Re flows as its foundation is microfluidics, which involves flows through micrometer dimensions. Since the characteristic length (and in most cases, the velocity too) is very small (order of 10-100 μm), the Reynolds number is very low. The flow physics changes drastically and becomes a lot more interesting at the microscale, owing to the various surface effects that start coming into picture such as surface tension, Marangoni effect, electric effects, etc. Microfluidic devices involving droplets and bubbles are now being used in various “Lab-on-a-chip” applications in which various chemical, biological processes and reactions are performed conveniently at the microscale [10-14], leading to exceptional progress in biomedical technology in the recent years. Another advantage of microfluidic flows is the ability to produce polydisperse droplets a lot more easily. Various methods have been developed for generating a continuous stream of microfluidic droplets [15-17]. These can be broadly categorized into three categories: droplet generation using co-flowing streams [18,19], droplet generation using cross-flowing streams in T-junction [20,21] and droplet generation using elongational flows (flow-focusing techniques) [22,23]. A particular term has been coined for this study of droplets at microscale- “Droplet Microfluidics”. It is essentially the study of low Re flows by taking various surface effects into account. As has been very aptly mentioned by H.A. Stone [24] in his review on microfluidics applications- “In particular, the most important issues are not “macro” versus “micro” but rather the relative magnitude

of various effects as characterized traditionally using dimensionless parameters.” Stone [24] also provided a list of various geometric (network connectivity, channel cross section and curvature, surface topography and porosity), chemical (wettability, surface charge, chemical affinity and ionic strength) and mechanical (hardness, elasticity) characteristics.

The effects of the geometric property, surface topography, have been reviewed in this paper. It refers to the shape of the surface and how it varies. This problem is studied by considering droplet flow through a constriction and showing how the flow can be manipulated in a variety of ways by altering the constriction properties. To understand what factors affect the drop flow through a constricted passage, it is essential to first understand the parameters which affect the flow in a straight channel, as those factors would anyways play a role in the former case too. This has been done in the next section. Following that, the surface topographic effects, which play an important role in determining the flow properties and bubble morphology, have been studied.

2. Flow through a straight channel

Analysis of droplet flow in a channel has been a topic of interest for long. The main factors which affect the multiphase phenomena and the flow properties (velocity profile and pressure drop) are the viscosity ratio (λ), the droplet size (a) and the Capillary Number (Ca). The viscosity ratio is the ratio of droplet viscosity (μ_2) to the surrounding fluid viscosity (μ_1), i.e. $\lambda = \mu_2/\mu_1$. The droplet size (a) is defined as the ratio of undeformed drop radius to the tube radius. The most important parameter is Capillary number, which measures the relative significance of viscous forces to the interfacial forces, the two major forces in low Re flow. Thus, the capillary number is defined as $Ca = \mu_1 V / \sigma$, where ‘ V ’ is the mean velocity of the suspending fluid, and ‘ σ ’ is the interfacial surface tension. The droplet and the surrounding fluid are assumed to be immiscible.

Initial studies in this area were focused on calculating the bubble velocity, the additional pressure drop across the bubble and the film thickness for different bubble fluids and suspending fluids [25-30]. The extra or the additional pressure drop is defined as the pressure drop over a distance extending into the undisturbed flow ahead and behind of the drop, minus the pressure drop in the normal Poiseuille flow over the same distance.

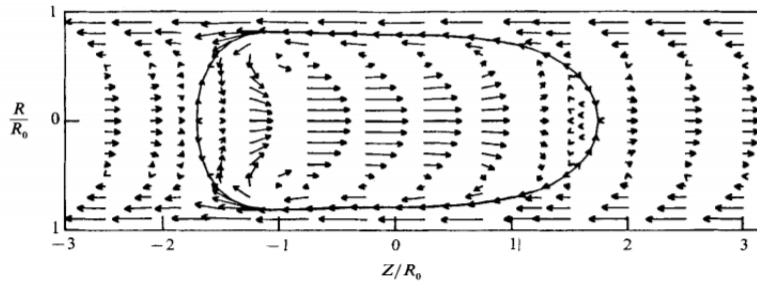


Figure 1: Velocity vector field in and around a drop for $a = 1.10$, $Ca = 0.10$, $\lambda = 0.19$. The velocities shown are relative to the drop velocity. Adapted from Martinez and Udell [34]. Copyright 1990 Cambridge University press.

Ho and Leal [31] did experimental studies to evaluate the extra pressure drop, velocity and shape of the drops for different viscosity ratios, capillary numbers and drop sizes by taking many different Newtonian as well as viscoelastic systems. Shen and Udell [32] evaluated velocities, pressure drop and film thickness in bubble flow using the finite-element method. Martinez and Udell [33] studied flow of long bubbles in capillaries using the boundary integral method and evaluated bubble velocities and

profiles. They continued their work to analyze axisymmetric motion of drops in circular tubes and computed drop speed and pressure drop for a wide range of capillary numbers, viscosity ratios and drop size [34]. Their work aptly summarizes and explains the effect of droplet flow in a straight channel very appropriately (Fig. 1 and 2).

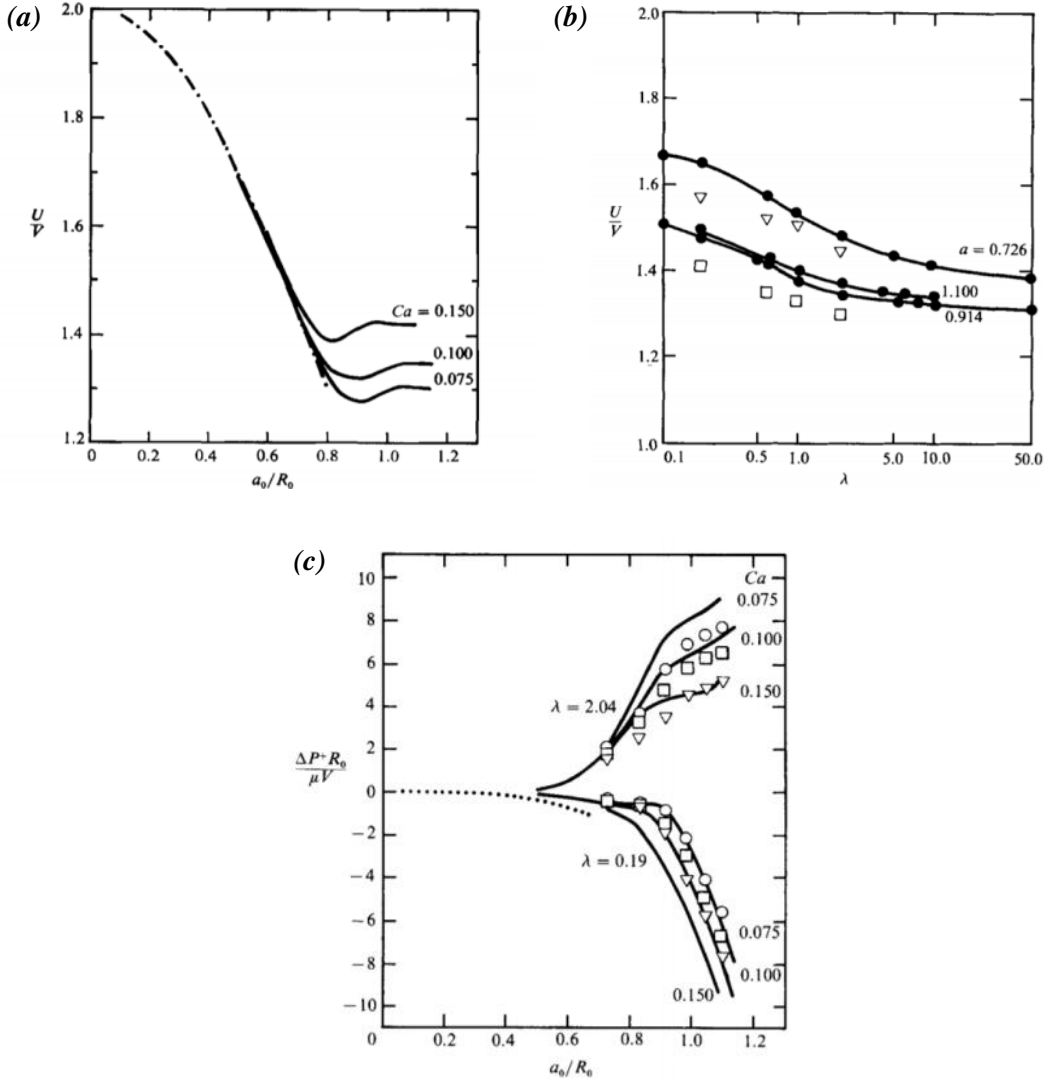


Figure 2: (a) Variation of drop velocity with the drop size for different capillary numbers, $\lambda = 10$; (b) Variation of drop velocity with viscosity ratio for different drop sizes; (c) Variation of additional pressure drop with drop size for different capillary numbers. Adapted from Martinez and Udell [34]. Copyright 1990 Cambridge University press.

The result of variation of each of the three major parameters has been described below:

2.1. Effect of capillary number

Capillary number gives an idea of the relative importance of the viscous forces being exerted on the drop by the surrounding fluid to the interfacial forces. If capillary number tends to zero, it implies that the viscous forces are negligible and hence, the droplet acquires a perfectly spherical shape where the surface tension balances the excess pressure gradient between the inside and outside of the drop (given by the Young-Laplace Equation).

If the capillary number increases, the deformation of the droplet increases (due to greater viscous forces) and hence the film thickness, which is the thickness of the fluid surrounding the droplet, increases. Also, since the drop is deformed more with an increase in Ca , the drop velocity also increases due to the drop being localized about the centerline, where the fluid velocities are higher [Fig. 2 (a)]. The additional pressure drop decreases with an increase in Ca [Fig. 2 (c)], but is also strongly dependent on the other two factors discussed below.

2.2. Effect of viscosity ratio

Viscosity ratio is the ratio of the droplet viscosity to the surrounding fluid viscosity. A larger viscosity ratio implies more resistance by the drop and hence a greater deformation. Also, greater resistance implies lesser velocities; hence the drop velocity decreases with the viscosity ratio [Fig. 2 (b)]. The effect of viscosity ratio on the pressure drop is very interesting. It has been observed that for viscosity ratios greater than 1, the additional pressure drop is generally positive, whereas for viscosity ratios lesser than 1, it is negative [Fig. 2 (c)]. The viscosity ratio, $\lambda = 1$ corresponds to droplet viscosity equal to the surrounding fluid viscosity and can be thought of as producing negligible additional pressure drop. Of course, this is a lot dependent on capillary number and the drop size. For example, for extremely small capillary numbers, the additional pressure drop is positive even for viscosity ratios less than 1.

2.3. Effect of drop size

The drop size is generally given with respect to the tube radius. A larger drop undergoes a greater deformation. The film thickness decreases with increase in drop size due to the bulkiness of the drop, so does the drop velocity [Fig. 2 (b)]. It has also been found that the magnitude of additional pressure drop increases with the size of the drop, for both viscosity ratios lower and greater than 1 [Fig. 2 (c)].

Olbricht and Kung [35] demonstrated that break-up of drops may take place even in a straight channel if the capillary number is too large. They termed the capillary number at which this process starts for a particular drop size and viscosity ratio as the critical capillary number. They inferred that critical capillary number increases with drop size and decreases with viscosity ratio.

3. Flow through channel with surface topography

Changing the surface geometry of the channel can lead to substantial changes in drop/bubble deformation and flow properties. The first study on droplet flow through a constricted passage was done by Olbricht and Leal [36], where they experimentally studied how the Capillary number, drop size and viscosity ratio affect the flow parameters such as drop velocity and the pressure drop as well as the drop morphology inside a constricted sinusoidal tube. Though the flow properties varied in the channel because of the constriction, the average values were found to follow the same general trends as for a straight channel flow.

One of the two main striking features which they found out for a constricted channel flow was that when the drop passes through the constriction, the pressure drop across the channel changes considerably and approaches a sinusoidal distribution for large droplet sizes. Though the average values may match the value in flow through a straight channel, the peak values of pressure drop (also called peak resistance), which occurs when the drop is flowing through the narrowest part of the constriction, is significantly higher than the average value (Fig. 3). Under conditions of imposed pressure gradient, extremely high peak resistances may lead to drop being retained at certain locations in the channel. Hence, the geometry needs to be modeled very carefully to get the desired results.

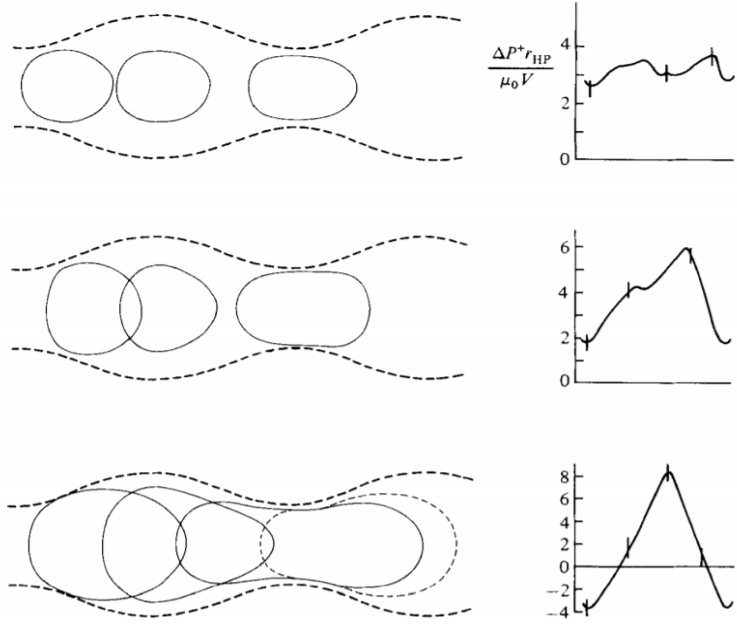


Figure 3: Variation in drop shape and additional pressure drop in flow through a constricted channel for increasing drop sizes (from top to bottom), $Ca = 0.043$. Notice how the additional pressure drop profile approaches a sinusoidal curve as the drop size increases. Adapted from Olbricht and Leal [36]. Copyright 1983 Cambridge University press.

The other important feature observed was that for the same parameters as a straight channel, drop break-up was observed in a constricted channel. This break-up has been a point of interest in many studies and has also been discussed in detail in subsequent sections.

Not only this, a constriction may also promote drop coalescence by allowing two parallel streams flowing through a constriction, which may usually not be possible in a straight channel. Yan et al. [37] studied this phenomenon and observed that this occurs at relatively lower capillary numbers since at higher capillary numbers, the enhanced deformation allows the drop to move through the constriction without undergoing coalescence.

Many other researchers have analyzed the effect of the above-mentioned parameters (Ca, a, λ) as well as the constriction parameters on the drop flow. Some reviews on flow through porous media [2, 38] have also been done, which give the reader a general idea of how a constriction affects the flow. An effort has been made to analyze the role of surface topography by looking at five major geometry parameters:

3.1. Effect of constriction shape:

The shape of the constriction plays a substantial role in determining the drop morphology and can be altered in many ways. The shape may be semi-circular, rectangular, trapezoidal, sinusoidal etc. The most common shape that has been studied is perhaps the sinusoidal geometry. The common form of the channel shape for flow through a sinusoidal converging/diverging tube is given by:

$$r(z) = r_a + \frac{d}{2} \sin(2\pi z / L) \quad (1)$$

where z is along the flow direction, r_a is the average radius of the tube, L is the length of the constriction and d is the depth of the constriction (maximum diameter, minus the minimum diameter). These parameters can be defined in a similar way for any kind of shape.

In addition to the studies by Olbricht and Leal (discussed in previous section), lot of studies have been done on drop flow through **sinusoidal constrictions**, including Tsai and Miksis [39] who analyzed this problem in detail using the boundary integral method. They also studied drop break-up by calculating the snap-off time of the drop in the constriction as well as the effect of capillary number on the snap-off. If the capillary number is too less, there is less fluid around the drop when it passes through the constriction (because of thinner film due to lesser deformation), so it takes longer for the film instability to develop. As the capillary number is increased, this instability is increased and snap-off starts taking place. But if the capillary number is too high, the snap-off doesn't take place, because of the large velocities which do not give time for instabilities to grow (though there is still a very minute portion of fluid which breaks off). Hence, there is a range of capillary numbers for which the breaking occurs (Fig. 4). They also studied how the drop size and the viscosity ratio affect the snap-off and concluded that a larger drop size promotes snap-off whereas the same is achieved by a lower viscosity ratio. The term ‘bubble’ has been used in the paper because of the viscosity ratios much less than 1.

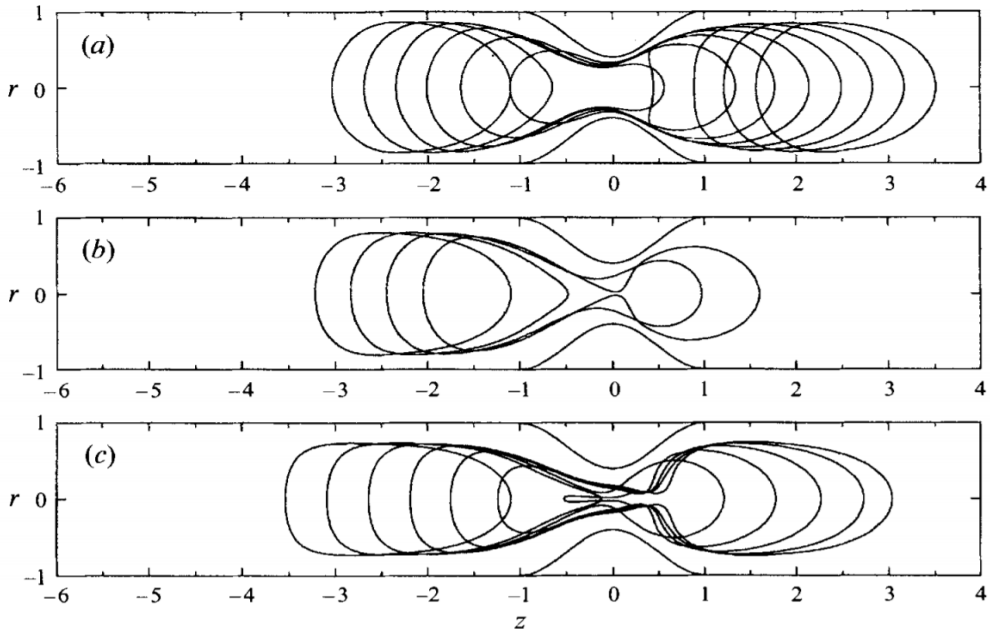


Figure 4: Effect of capillary number on snap-off of a bubble in a sinusoidal constriction, $a = 0.9$, $\lambda=0.001$: (a) $Ca = 0.05$; (b) $Ca = 0.1$; (c) $Ca = 0.2$. Observe that snap-off occurs only for $Ca = 0.1$. Adapted from Tsai and Miksis [39]. Copyright 1994 Cambridge University press.

Another type of constriction shape which has been studied includes **rectangular geometry**. Nath et al. [9] analyzed motion, deformation and behavioral changes of EMT cancer cells passing through rectangular micro capillaries to know the exact mechanism of cancer spreading, which is not known precisely yet. They studied how the cancer cells invade the blood capillaries via basement membrane and how the motion of cells through the blood micro capillaries takes place. For the former case, they had constrictions having gaps in the range of $10\text{--}15 \mu\text{m}$ and for the second case, the gap was $7 \mu\text{m}$. They calculated the deformation index, entry time and velocity of the cells for different gap sizes and cell sizes. Such parameters are important to understand the ability of cancer cells to move through the

constricted capillaries. In this case, cells can be considered equivalent to droplets as they too undergo deformation and can be modeled as different phase than that of surrounding fluid i.e. blood. It was found that the cells are deformed to a great extent inside the micro channel, which is still prominent after they come out of the constriction (Fig. 5). This property of having enhanced deformation can be used to study the elastic properties of protein networks in the blood as had been mentioned in one of the applications in the beginning [10]. It is also to be noted that it is not necessary that drop break-up will not happen in rectangular constrictions since it depends on a lot of other parameters like capillary number, as has been seen earlier. A very large capillary number may indeed lead to a break-up.

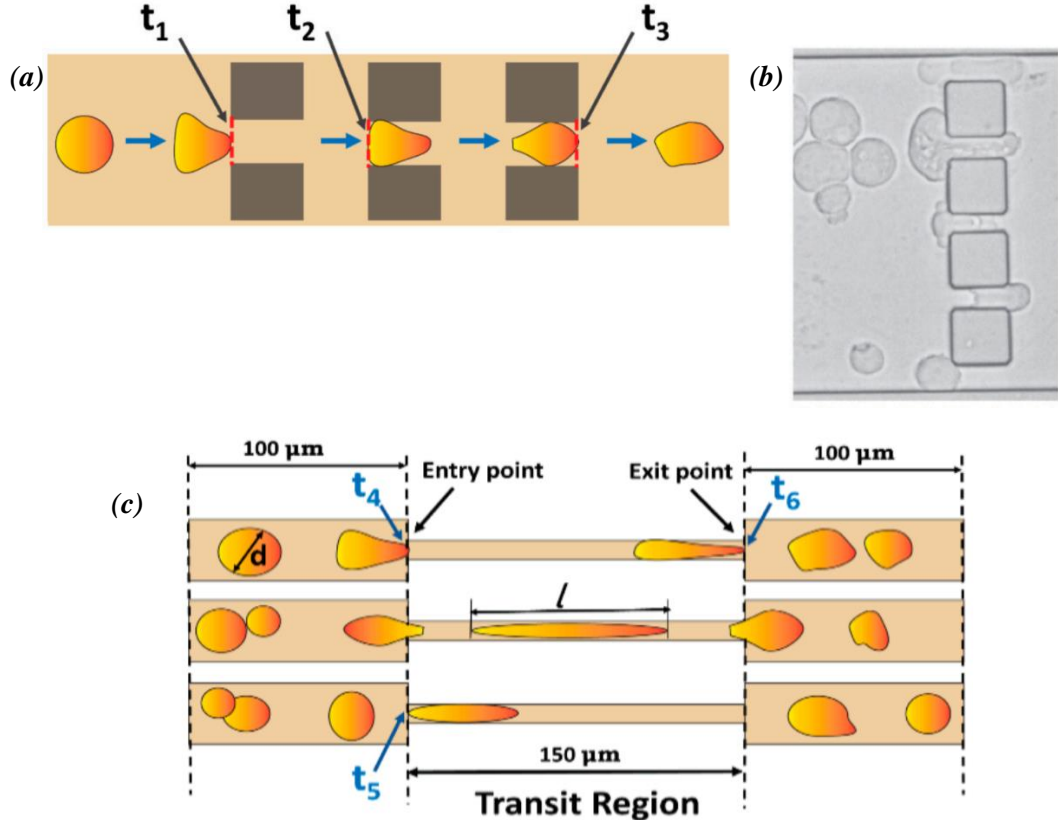


Figure 5: (a) & (b) Deformation and elongation of cells in rectangular constrictions resembling the basement membrane. Gap size is in the range of 10–15 μm ; (c) Deformation and elongation in constrictions resembling microcapillaries. Gap size is 7 μm . Adapted from Nath et al. [9]. Copyright 2019 Multidisciplinary Digital Publishing Institute.

In addition to elongation, some interesting shapes have also been observed through a rectangular constriction for a smaller drop size and higher velocities. Chen et al. [40] observed crescent moon shaped bubbles coming out of a rectangular constriction (Fig. 6). The reason for such a shape was that as the bubble approaches the constriction, the flow converges, and the bubble attains a higher velocity due to its small size and is elongated in the flow direction. After passing through the constriction, the velocity of the front part starts reducing in the diverging section. The back of the bubble is still travelling at a higher velocity, giving the crescent moon shape.

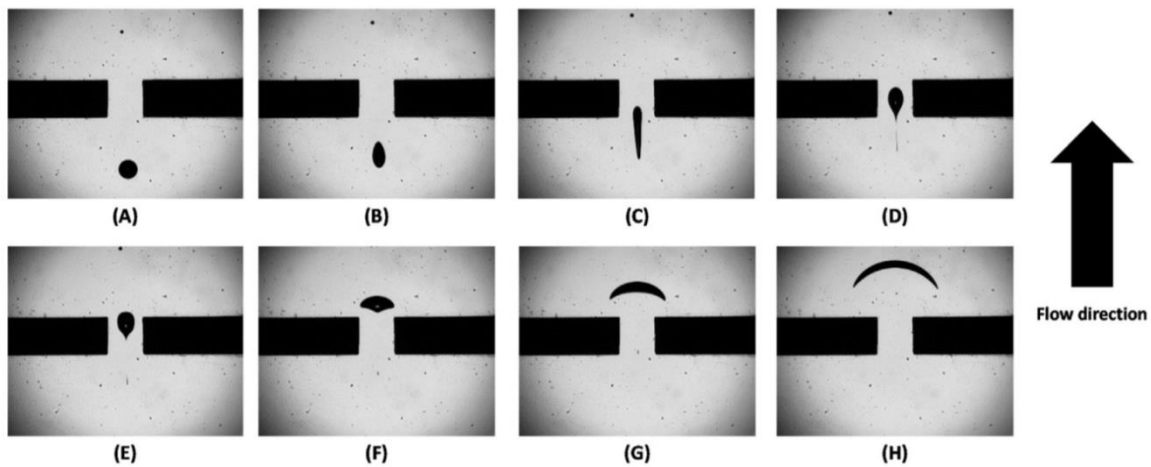


Figure 6: Evolution of a spherical bubble of initial radius $745\text{ }\mu\text{m}$ passing through an orifice. Continuous phase flow velocity = $7.85\text{ mm}^3/\text{s}$. Adapted from Chen et al. [40]. Copyright 2019 Elsevier Ltd.

Drop flow has also been studied through a constriction resembling a **trapezoid**. Cunha et al. [41] evaluated the mobility reduction factor and drop shapes for flow in such a geometry. The mobility reduction factor is a representative of the pressure and drop flow-rate relation in the flow and increases with decrease in maximum additional pressure drop. The drop shapes shown in the paper resemble those in the previous case of rectangular geometry (Figure 6). This is because base length is taken to be very large due to which the drop is elongated and hence the trapezoid legs seem to play no significant role. It can be studied further till what ratio of leg length to base length will such a deformation be observed and when will snap-off start taking place. It is also observed that the drops elongate in the flow direction before the constriction and in the orthogonal direction after the constriction. Cabral and Hudson [42] also observed flow in trapezoidal-type geometry and a similar evolution of drop shapes can be seen. An important phenomenon that has been observed in similar geometries is drop coalescence, where the drop is stopped at the constriction, allowing the succeeding drop to come and merge with it [10, 43]. This phenomenon has also been discussed in subsequent sections.

Zinchenko and Davis [44] studied flow in a porous media using the boundary integral method where the porous media structure was modelled using either spheres or disks. For example, an arrangement of two spheres, placed at a certain distance, is used and the drop passes symmetrically through them. This can thus be viewed as flow through a **semi-circular constriction**. The drop deforms perpendicular to flow direction as expected but some interesting shapes are obtained if the results are analyzed in 3-D. It is seen that the drop surface starts becoming dimpled (Fig. 7, $t=20$), which would have not been visible, had the drop been seen in 2-D. The dimple starts to disappear when the drop comes out of the constriction and the drop takes the form of an elongated sphere, and ultimately returns to a spherical shape further downstream. Other studies have also been done on drop flow in semi-circular constrictions, which have been discussed in sections 3.2 and 3.5.

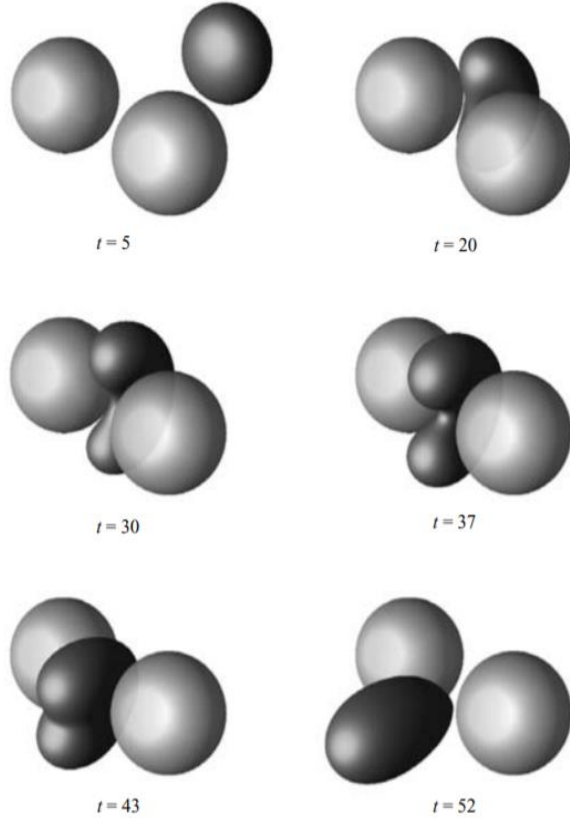


Figure 7: Evolution of drop shape while passing through a two-sphere constriction for $Ca = 0.63$, $a = 0.9$, $\lambda = 4$ for different time-steps. Observe how the drop surface starts becoming dimpled while approaching the constriction. Adapted from Zinchenko and Davis [44]. Copyright 2006 Cambridge University press.

Numerical studies of drop deformation have also been done in a **hyperbolic constriction** by Khayat et al. [45]. They calculated the deformation parameter, α , which is defined as the ratio of difference in current perimeter and the initial perimeter of the drop, to its initial perimeter. They observed that the deformation was symmetrical before and after the constriction, and α obtained a peak at the center of the constriction, thus corresponding to maximum deformation. This was for the case of a drop placed symmetrically initially. Droplets placed off-axis initially, in addition to undergoing rotation, also retain deformation while coming out of the constriction (Fig. 8), unlike the symmetrical case. Study on drop flow on a hyperbolic constriction has also been done by Leyrat-Maurin and Barthe-Biesel [46], who analyzed the effects of capillary number and drop size on parameters such as drop shape and flow rate.

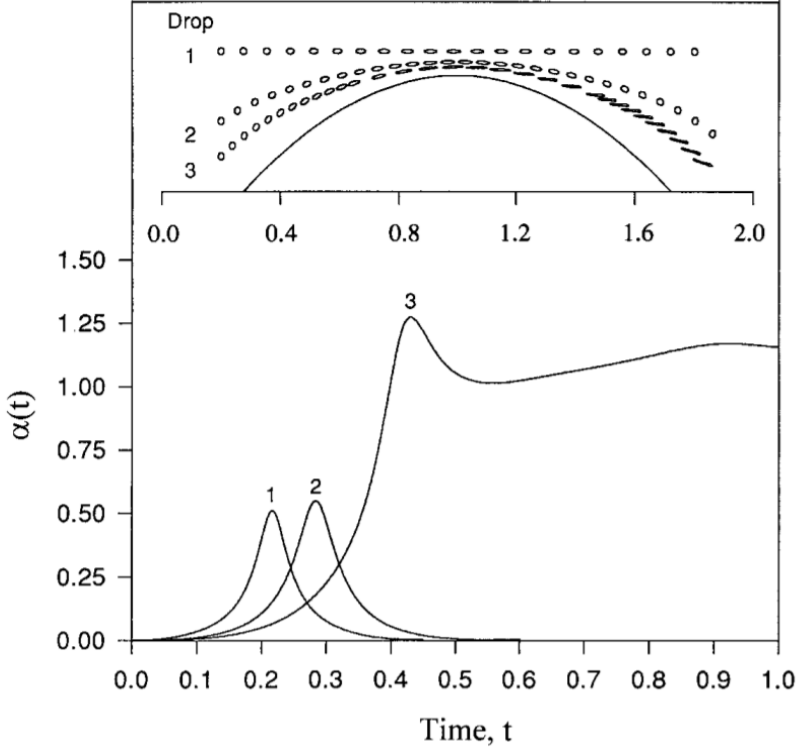


Figure 8: Drop shapes and deformation for symmetrical and unsymmetrical initial positioning of drops, $a = 0.02$, $\lambda = 4$. Observe that the droplets placed symmetrically (marked by 1) retain their shape, while the droplets placed off-axis (3) have high deformations on coming out of the constriction. Adapted from Khayat et al. [45]. Copyright 1999 Elsevier Science Ltd.

Roca and Carvalho [47] analyzed drop flow through a geometry consisting of **three tangent arcs of circles** and showed that the mobility reduction factor decreases with decrease in capillary number and increase in viscosity ratio and drop size. The drop shapes seemed to resemble those in sinusoidal geometries because of shape similarity.

Though it has been seen that different shapes of geometries can lead to different properties and drop shapes, the effects of a particular shape may not be unique to it. It is just that such results have been observed for that shape for a given set of parameters, which may differ in different papers. While this is true, it is also true that certain constriction shapes are more suited to particular applications, as has been discussed above. Thus, it can be an interesting area to study how the constriction shape specifically changes the flow behavior and drop shape, when all other parameters are kept constant.

While closing this section, it is worth mentioning that in addition to surface shape, the effects of shape of the cross-sectional area have also been studied, which are not being discussed in detail in this paper. For example, Gauglitz et al. [48] studied bubble break-up in a square constricted capillary, whereas Ransohoff et al. [49] studied the effects of different types of noncircular geometries such as triangular, rectangular etc. on bubble snap-off. Kovscek and Radke [50] also studied gas bubble snap-off under pressure driven flow in noncircular capillaries.

3.2. Effect of constriction ratio:

The constriction ratio refers to the ratio of maximum diameter to the minimum diameter (also known as throat diameter) in the tube. It is also sometimes referred to as the constriction depth or the constriction gap. For a converging/diverging channel, the constriction ratio (C) is defined as:

$$C = \frac{R}{R-d} \quad (2)$$

where R is the radius of the channel and d is depth of the constriction.

Tsai and Miksis [39] evaluated the bubble shapes keeping all other parameters same and varying only the constriction depth in a tube of radius 1 (all values have been reported in non-dimensional units with respect to channel radius). They observed snap-off in a constricted channel of depth 0.6 (constriction ratio = 2.5) whereas no such snap-off was observed in a constriction having a depth 0.5 (constriction ratio = 2) as shown in Fig. 9. This shows that a greater constriction ratio promotes the snap-off of the bubble due to increased pressure and instability in the narrower constriction.

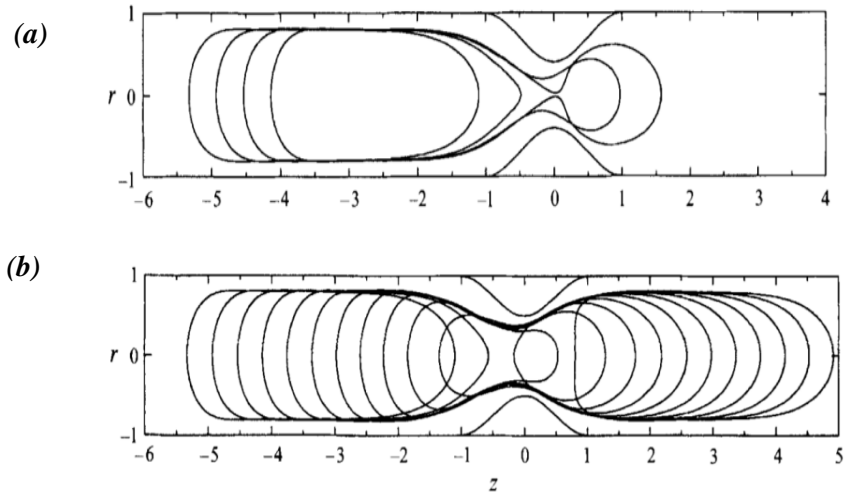


Figure 9: Effect of constriction ratio on snap-off of a bubble with $a = 1.2$, $\lambda = 0.001$, $Ca = 0.1$: (a) Constriction ratio = 2.5; (b) Constriction ratio = 2. Observe the snap-off taking place in the first figure. Adapted from Tsai and Miksis [39]. Copyright 1994 Cambridge University press.

Martinez and Udell [51] used the boundary integral method to analyze flow through two different sinusoidal tubes having periodic constrictions with constriction ratios 3 and 1.8 respectively. The maximum pressure drop was positive for both the tubes and it was found to be greater than in the narrower tube (constriction ratio = 3), showing that the pressure in the constriction is more for higher constriction ratio tubes, thus implying a greater resistance [Fig. 10 (c) and (d)].

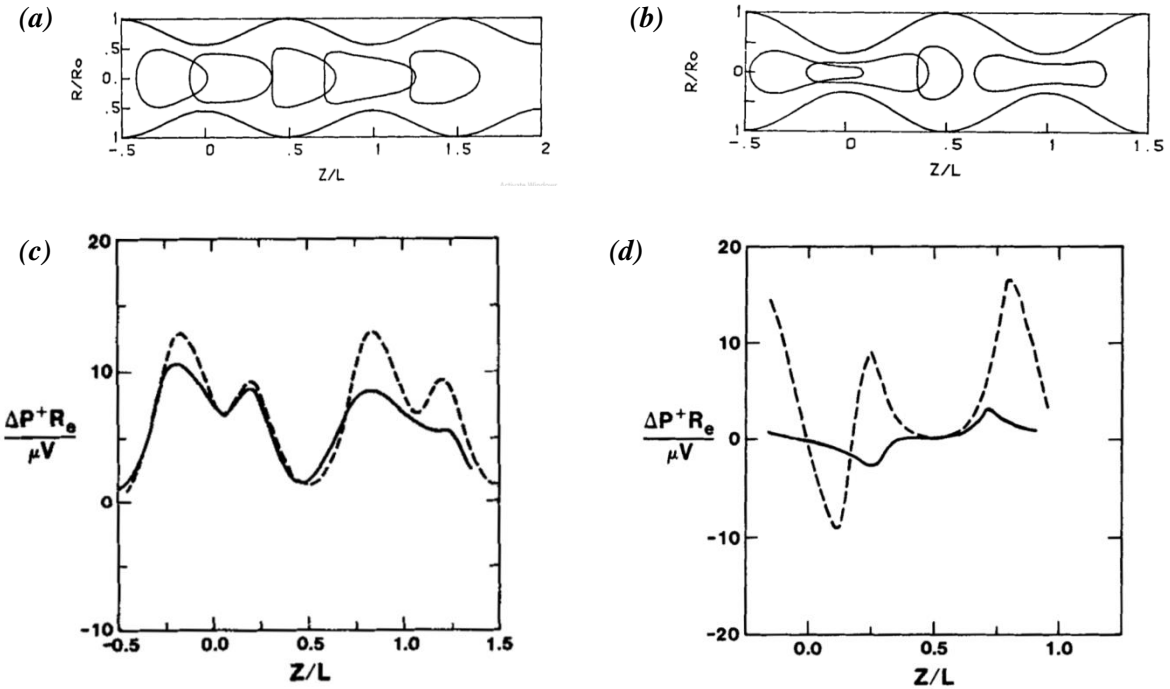


Figure 10: (a) Drop shape evolution in tube with constriction ratio 1.8, $a = 0.76$, $Ca = 0.5$, $\lambda = 10$; (b) Drop shape evolution in tube with constriction ratio 3, $a = 0.9$, $Ca = 0.5$, $\lambda = 1$; (c) Additional pressure drop in tube with constriction ratio 1.8; (solid line) $a = 0.76$, $Ca = 0.5$, $\lambda = 10$; (dashed line) $a = 0.76$, $Ca = 0.083$, $\lambda = 7.5$; (d) Additional pressure drop in tube with constriction ratio 3, $a = 0.90$, $\lambda = 1$, (solid line) $Ca = 0.5$, (dashed line) $Ca = 0.083$. Adapted from Martinez and Udell [51]. Copyright 1990 American Physical Society.

They also observed droplet deformation in the tubes though it cannot be compared directly as the other set of influencing parameters (Ca , λ , a) were different for the two cases. But it can be easily inferred that a greater constriction ratio implies more drop deformation [Fig. 10 (a) and (b)]. Higher constriction ratios also imply a greater tendency of drop break-up due to higher pressures and deformations. Due to the same reason, a decrease in drop speeds with increase in constriction ratio was also reported, though it is also a lot more dependent on drop size. Hence, one needs to carefully optimize all the given parameters at hand to match the flow best suited to one's requirements.

Nath et al. [9] also discussed the effect of constriction gap on various important parameters (Fig. 11). As mentioned in the previous section, they studied the behavioral changes in EMT cancer cells passing through rectangular microcapillaries. For a constant cell size, the deformation index (ratio of drop length to its width) and the entry time increase with decreasing gap size due to enhanced deformations. Due to the same reason, the cell velocity in a broader gap is more. The deformation index increases with increasing cell size. As a greater cell size corresponds to more bulkiness, the entry time increases with the increase in cell size, whereas the transit velocity decreases.

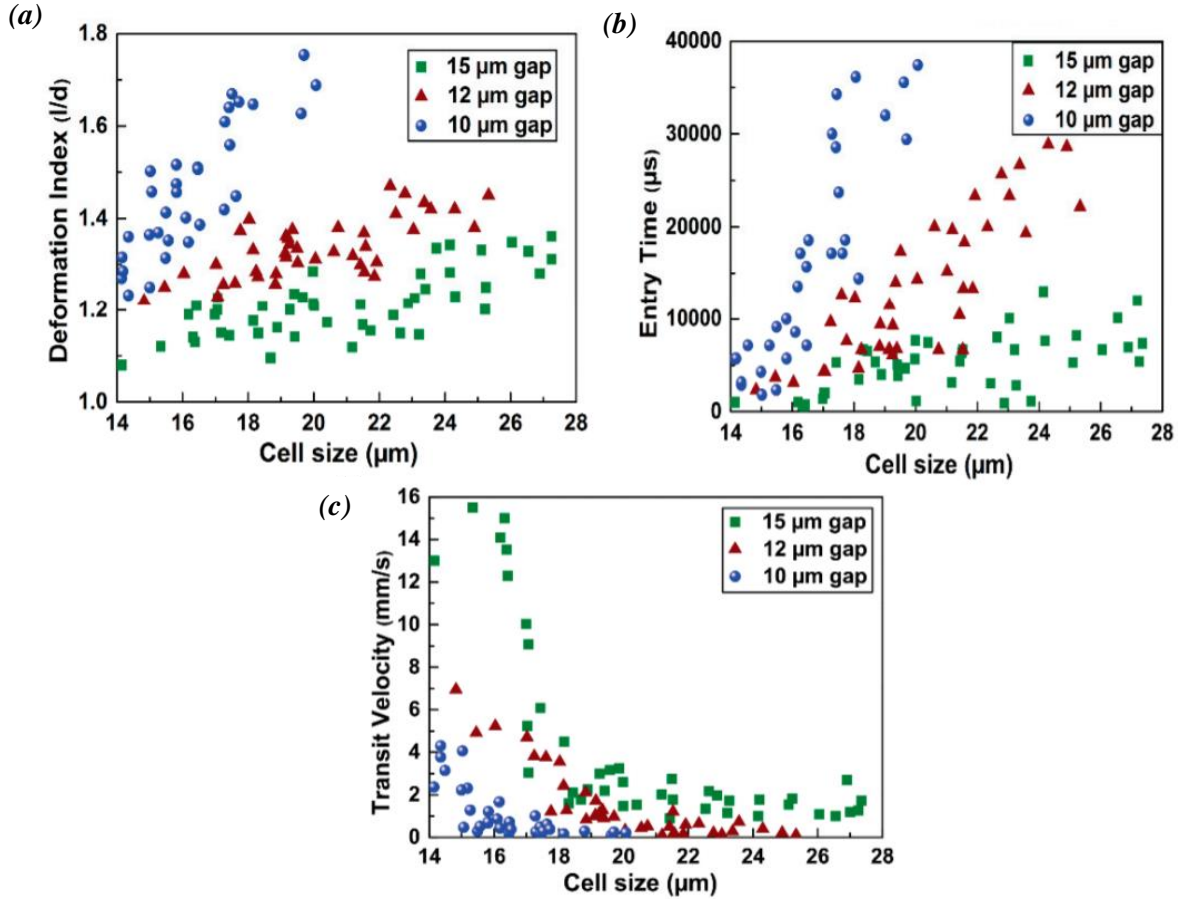


Figure 11: Effect of cell size and gap size on (a) Deformation index; (b) Entry time; (c) Transit velocity. Adapted from Nath et al. [9]. Copyright 2019 Multidisciplinary Digital Publishing Institute.

Ratcliffe et al. [52] studied the effects of gravity on the squeezing of a deformable drop through a ring constriction. The circular ring can be thought of as a constriction with a semi-circular boundary. They varied the cross-section-to-hole radius ratio, which can be related to the constriction ratio: a greater cross-section-to-hole-ratio implies a smaller hole radius relative to the cross-section, which corresponds to larger constriction ratio. They found out that on decreasing the cross-section-to-hole ratio, a transition takes place from squeezing to dripping. This means that instead of “squeezing” through the constriction, the drop starts “dripping” around the constriction for lower cross-section-to-hole ratios (or higher constriction ratios), as shown in Fig. 12. This seems to be true in general and may apply to any case involving a high constriction ratio, in which the drop may not pass through the constriction and get deposited at the walls before it. Similar results were observed by Bordoloi and Longmire [53], who studied the motion of gravity-driven deformable drops through a circular confining orifice. They also observed drop break-up for moderate constriction ratios, when neither dripping (or capturing) nor squeezing (or release) occurs.

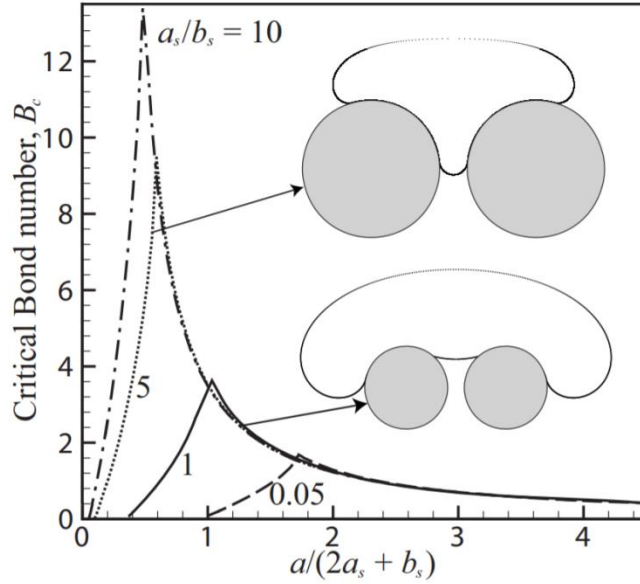


Figure 12: Variation of critical bond number (the minimum bond number below which drop trapping occurs) with cross-section radius (a_s), drop radius (a) and hole radius (b_s). Observe that on decreasing the a_s/b_s ratio from 5 to 1, a transition from squeezing to dripping occurs. Adapted from Ratcliffe et al. [52]. Copyright 2010 American Physical Society.

Effect of constriction ratio has also been numerically analyzed by Patel et al. [54], though their study is not in the low Re flow regime and includes inertial effects. The effects of gravity have also been taken into account by varying the Bond number (Bo). Nevertheless, a good understanding is obtained on how the drop shape evolves with changing constriction ratio (Fig.13). They also mentioned that the aspect ratio (ratio of bubble width to its length) increases for very high constriction ratios as the bubble starts elongating due to formation of low-pressure zones near its ends. Like other cases, the bubble velocity was found to decrease with increasing constriction ratio.

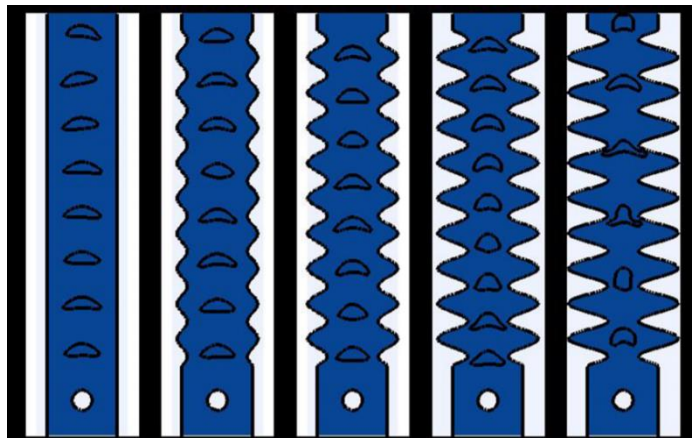


Figure 13: Evolution of drop shape in constricted channels with increasing constriction ratio from left to right at $Re = 300$ and $Bo = 5$. Adapted from Patel et al. [54]. Copyright 2019 American Physical Society.

Thus, to conclude this section, it can be said that a greater constriction ratio corresponds to greater deformations, higher pressures, higher resistances and lower velocities (for larger drop sizes). A higher

constriction ratio also implies a greater tendency for the droplet to snap-off. Thus, the constriction ratio can be modeled to promote phenomenon of drop break-up. Interesting shapes involving elongation are also observed for narrower channels.

3.3. Effect of phase angle between constrictions:

Phase angle refers to shift in phase between the periodic constrictions at the upper-wall and the lower-wall. The cases analyzed above have zero phase angles. The phase angle can vary from 0° to 360° . A phase angle of 360° implies a shift by one full constriction length and hence is the same as 0° . Having non-zero phase angles can change the flow parameters significantly. It can also have a considerable effect on the drop shape as shown below.

Sauzade and Cubaud [55] studied the effect of phase angle on the bubble shapes. The end of the upper constriction points to the middle of the lower constriction, thus indicating a phase angle of 180° . The constriction in this case resembles a triangular shape, though there is some curvature too. It can be observed that bubbles start acquiring velocities in vertical direction as well as asymmetrical shapes with respect to the horizontal axis (Fig. 14). Bubbles also seem to attain quite intriguing shapes, such as pointed triangles and zig-zag quadrilaterals.

Though the velocities inside the bubbles have not been computed, this type of motion hints that this type of geometry may enhance mixing of liquids inside the confined bubbles. Mixing requires generation of vortices within the complete bubble so that various chemical and biological reactions can take place. In flat channels having zero phase, efficient mixing is not possible since the vortices are formed in separate halves of the bubbles. Though these vortices may mix the contents of each half, there is no fluid exchange between the two halves. Thus, as of now, special zig-zag, serpentine-like, rectangular corners and other similar channels are employed to enhance mixing [10, 56-59]. If it would be possible to ensure mixing just by altering the phase angle, it would indeed form a very fascinating application to be explored further.

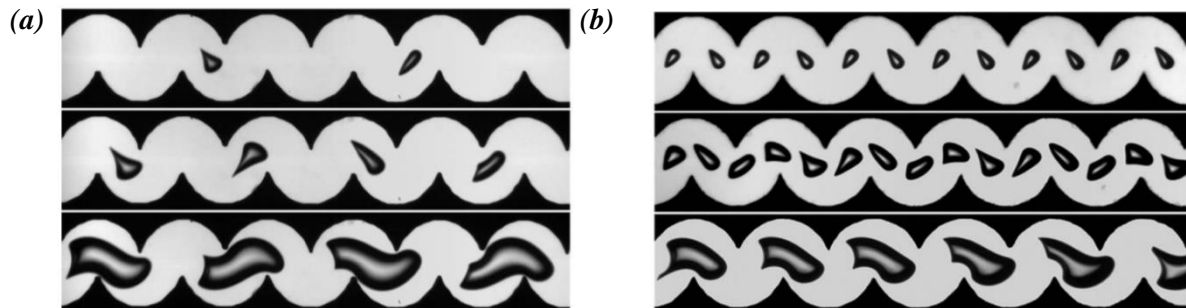


Figure 14: Effect of non-zero phase angle on bubble shapes in highly viscous oils with increasing gas volume fraction from top to bottom, (a) Air bubbles in 1,000 cS oil; (b) Carbon dioxide bubbles in 10,000 cS oil. Adapted from Sauzade and Cubaud [55]. Copyright 2014 American Physical Society.

Patel et al. [54] also observed the effect of phase angle in an inertial flow (Fig.15). The effects are not as prominent as the above case because of the lesser drop size and greater constriction gap. They found that changing phase angle also changes the bubble velocities and the aspect ratios. The maximum velocity as well as the velocity fluctuations decrease with increasing phase angle. The maximum values of aspect ratio increased with increasing phase angle, while the fluctuations in the same were found to show a decrease. Also, the phase angles in their paper have been reported with a phase shift of 180° from how it has been defined in this paper.

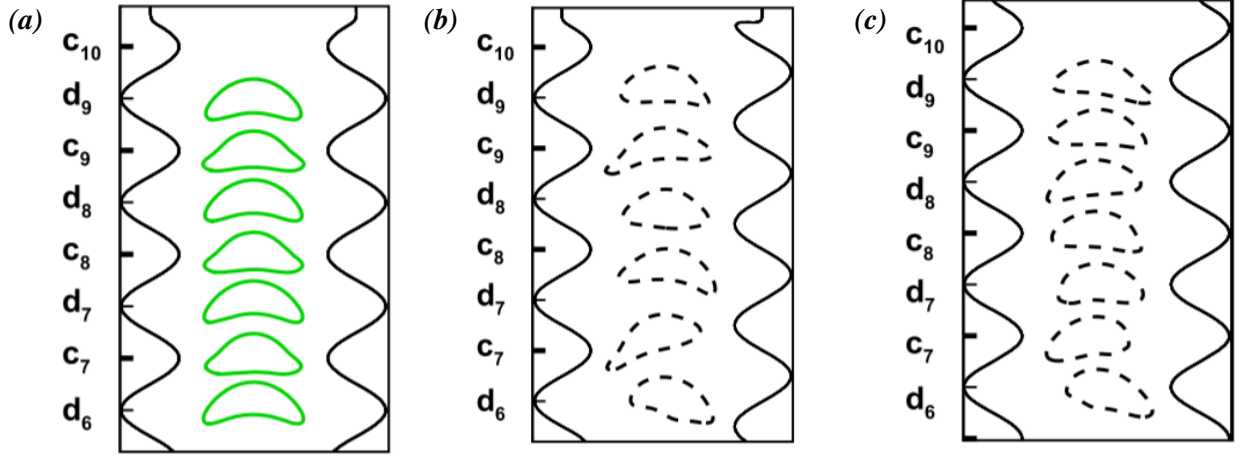


Figure 15: Effect of phase-angles on drop morphology in an inertial flow with $Re = 300$ and $Bo = 5$, phase angle (a) 0° ; (b) 90° ; and (c) 180° . Adapted from Patel et al. [54]. Copyright 2019 American Physical Society.

3.4. Effect of length of the constriction

Tsai and Miksis [39] computed the effects of length of constriction on the bubble flow (Fig. 16). They took three different values of constriction lengths- 1.5, 2 and 4 (all values in non-dimensional units with respect to channel radius). While snap-off was observed in all the three cases, there was significant difference in snap-off parameters, such as the snap-off time (the time taken for the bubble to break-up) and the snap-off bubble radius (the radius of the front bubble after snap-off), which have been tabulated below:

Constriction Length (l)	Time taken to snap-off (τ)	Bubble Radius (b_r)
1.5	0.68	0.77
2	0.42	0.64
4	0.45	0.68

Table 1: Effect of constriction length, snap-off time and bubble radius after snapping-off. All values are in non-dimensional units. (Values taken from Tsai and Miksis [39]).

Both snap-off time and bubble radius seem to follow a decreasing-increasing trend with increasing constriction length, implying that there may be minima somewhere in between. But, since the number of observations is too less, nothing concrete can be established, and this remains another area which can be studied further to get meaningful insights into this multiphase problem.

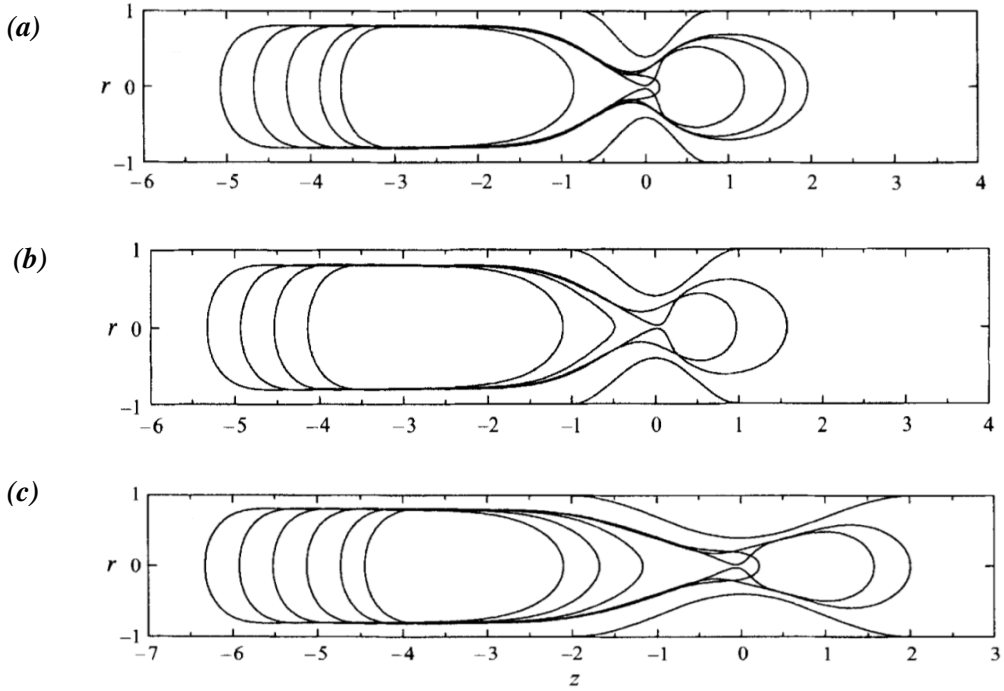


Figure 16: Evolution of an initially steady shape bubble with $a = 1.2$, $\lambda = 0.001$ and $Ca = 0.1$ for (a) $l = 1.5$; (b) $l = 2$; and (c) $l = 4$. Adapted from Tsai and Miksis [39]. Copyright 1994 Cambridge University press.

3.5. Effect of periodicity and spacing between the constrictions

This problem has not been studied quite thoroughly, but a few inferences can certainly be made based on some observations. Most of the zero phase angle cases that have been seen above only consider a single constriction. Having multiple constrictions, even in a zero phase angle case, can lead to interesting results. Sauzade and Cubaud [55] studied the motion of drops in corrugated channels with semi-circular periodic constrictions. They observed many interesting drop shapes varying throughout the geometry and periodic in nature (Fig. 17). When the flow velocity of the bubble is increased, the bubbles are seen to deform from out of phase to in-phase mode. In the out of phase mode, the bubble is less deformed and shows periodicity in shape after every third periodic constriction whereas for in-phase mode, the bubble is elongated and shows periodicity in shape after every alternate constriction. Martinez and Udell [51] also observed different periodic shapes in periodic constriction channels (Fig. 10 in section 3.2).

The parameter which will play a major role in periodic constrictions having a fixed shape and length would be the spacing between the constrictions. For the above cases, the spacing between two consecutive constrictions was negligible as the constrictions almost touched each other. A single constriction can be visualized as a constriction with the spacing tending to infinity. Having some fixed spacing and manipulating flow within it can lead to interesting phenomena like drop coalescence, as shown next.

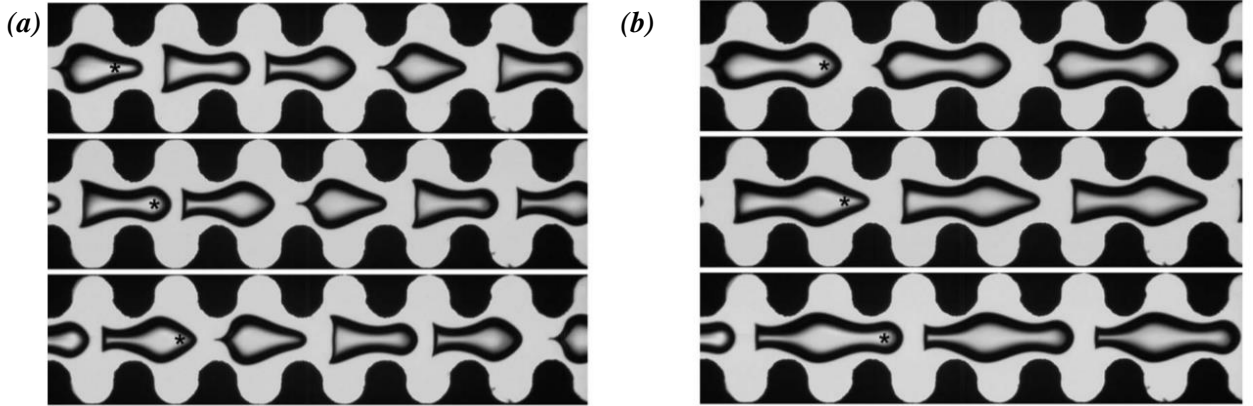


Figure 17: Time-series of elongated air bubbles flowing with an oil of viscosity 103 cS in a mildly deformed microchannel. Different initial liquid-gas flow conditions can lead to different phase shifts: observe that bubbles in (a) are out of phase (lower velocity), whereas bubbles in (b) are in-phase (higher velocity). Adapted from Sauzade and Cubaud [55]. Copyright 2014 American Physical Society.

Seemann et al. [10] in their review on droplet microfluidics summarized how droplet coalescence can take place by various mechanisms. They also emphasized the use of channel geometry and showed how different types of geometries can lead to drop coalescence. In [Fig. 18 (a)], the drop has been stopped by enlarging the channel and providing appropriate spacing, thus allowing the coming drop to merge into it. In [Fig. 18(b)], adequate spacing has been provided between the constrictions, which allows the continuous phase to flow around the droplet and slow it down. This allows the succeeding drop to merge into the first one. This type of drop coalescence by varying the geometry is indeed a very fascinating application and has also been studied by many researchers [60-64].

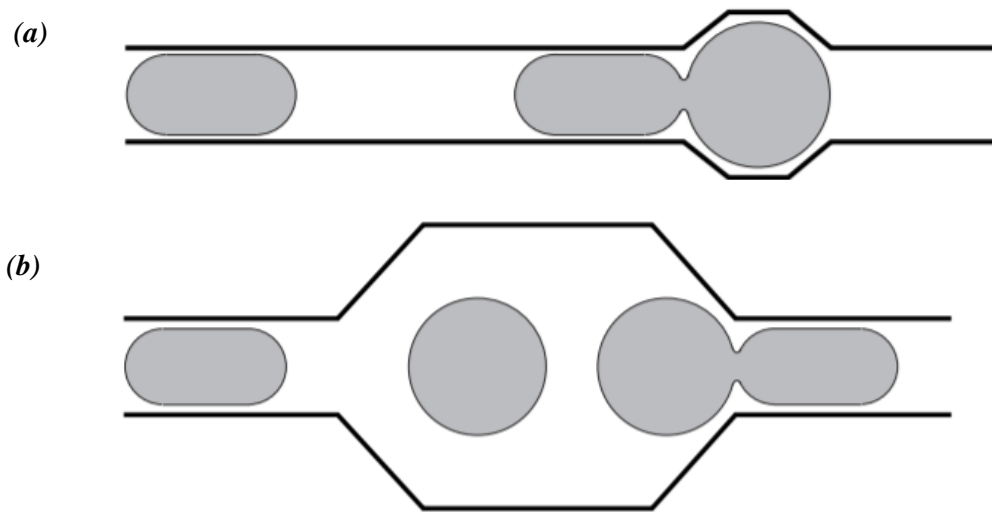


Figure 18: Drop coalescence by (a) stopping the droplet in between the spacing between the two constrictions; (b) slowing down the droplet and allowing the succeeding droplet to merge into it. Adapted from Seemann et al. [10]. Copyright 2012 IOP Publishing.

Thus, it can be inferred that periodicity and spacing not only lead to interesting drop shapes in the flow but also play a major role in the phenomenon of coalescence.

4. Scaling analysis for multiphase flow through constricted passage

From the above review of papers, it is found that a more systematic study of constricted passage is necessary to explore the various application of drop/bubble deformation.

Fig. 19 shows the different shapes of constriction geometry studied so far:

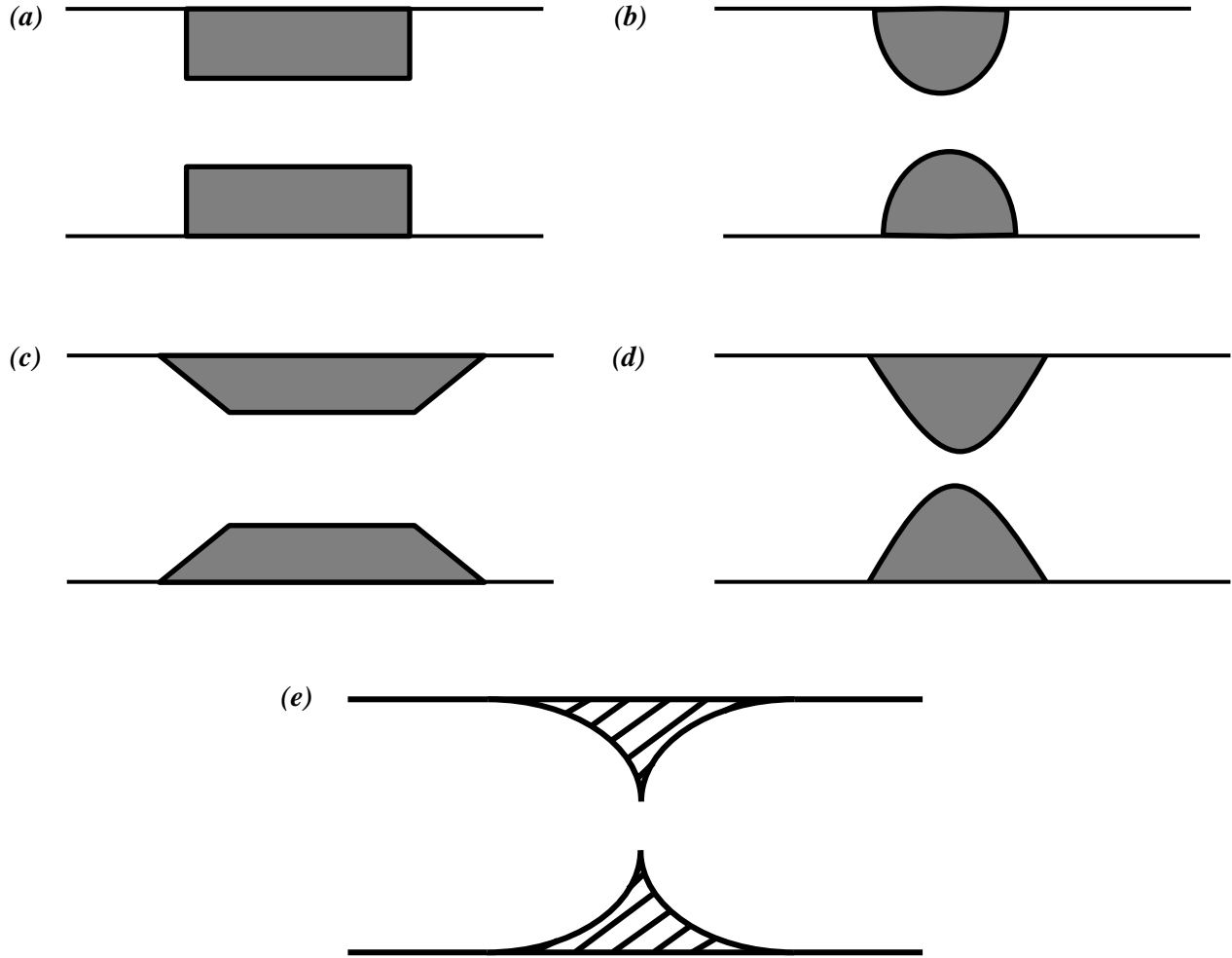


Figure 19: Schematic illustrating four different constriction shapes: (a) rectangular; (b) semi-circular; (c) trapezoidal; (d) sinusoidal; and (e) curved triangular geometry.

Now, we aim to list the various non-dimensional parameters involved in the process. The main governing forces in the flow are the viscous forces, interfacial forces and the gravity (only if density difference is present). It has already been seen that the pressure drop, flow speed, drop shape and multiphase phenomena depend upon a lot of parameters. A schematic of typical periodic constriction is shown in Fig. 20 with different length scales leveled. The main parameters that have been identified are the drop-radius (a'), mean Poiseuille flow velocity (V), radius of the channel (R), surface tension (σ), viscosity of suspending fluid (μ_1), viscosity of the drop (μ_2), density difference between the two fluids

$(\rho_c = \rho_2 - \rho_1)$, depth of the constriction (d), length of the constriction (L), spacing between two consecutive constrictions (S), and the phase shift (P). Phase shift is the distance between the starting of the upper constriction and the corresponding lower constriction. This parameter will give an idea of the phase angle. In total, there are eleven-dimensional parameters having units consisting of three independent fundamental physical quantities - length, mass and time. Thus, according to Buckingham π Theorem, eight non-dimensional numbers are obtained, namely, capillary Number, $Ca = \mu_1 V/\sigma$, Bond Number, $Bo = \rho_c g R^2/\sigma$, viscosity Ratio, $\lambda = \mu_2/\mu_1$, spacing parameter, $\bar{S} = S/R$, length parameter, $\bar{L} = L/R$, constriction gap parameter, $\bar{D} = d/R$, drop size, $\bar{A} = a'/R$, and the phase shift, $\bar{P} = P/R$. Thus, the non-dimensional pressure drop ($\Delta PR/\mu_1$), non-dimensional velocity (u/V) and the drop shape are a function, $f(Ca, Bo, \lambda, \bar{S}, \bar{L}, \bar{D}, \bar{A}, \bar{P})$, of these eight quantities.

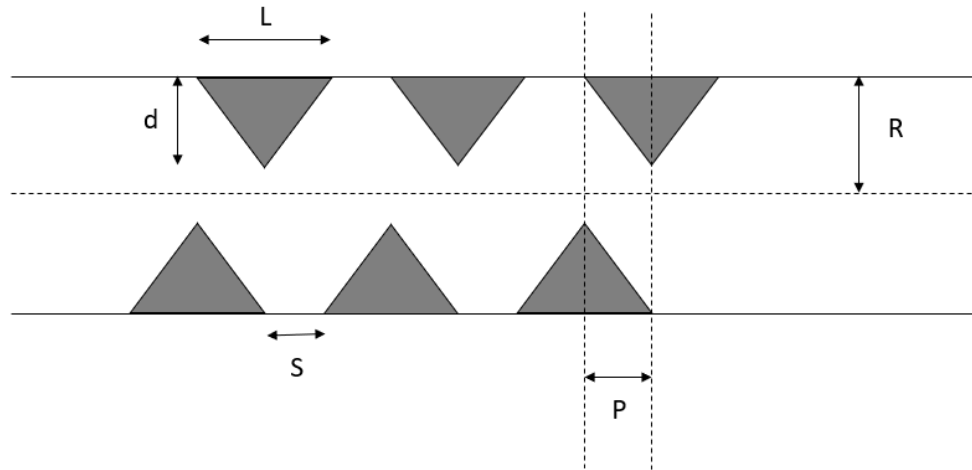


Figure 20: Schematic depicting the geometry parameters in periodic triangular constrictions.

5. Summary and Discussion

In this paper we have studied the recent progress regarding the drop/ bubble morphology as it flows through constricted passages. Since different people have calculated different parameters, for most of the cases it was difficult to analyze how changing only a particular geometry parameter affects the morphology.

Drops/bubbles deformation, velocity and pressure gradient across the straight micro channel are dependent on the droplet to channel radius ratio, viscosity ratio and the capillary number. Reviews show that the primary forces involved in such flows are the interfacial force which tends to deform the drop/bubble surface and the counteracting viscous force.

Analysis of surface topography is done based on constriction shape, constriction ratio, phase angle between constrictions, length of the constriction and constriction periodicity. Having some fixed spacing and manipulating flow within it can lead to interesting phenomena like drop coalescence and mixing. In case of wavy channel, in certain circumstance there could be very high pressure drop which may lead to drop being retained at certain locations in the channel. To avoid such situation, proper investigation is needed. Systematically investigating how the constriction shape specifically changes the flow behavior and drop shape, when all other parameters are kept constant is necessary.

For a greater constriction ratio, snap-off of the bubble is observed due to increased pressure and instability in the narrower constriction, but again the effect of constriction shape along with constriction ratio is not studied. The trends for both snap-off time and bubble radius with change in increasing constriction length also indicates a need to find the transition length. Similarly with change in phase angle for different shaped constriction, it would be interesting study to explore the possibility of mixing.

Periodicity and spacing not only lead to interesting drop shapes in the flow but also play a major role in the phenomenon of coalescence. 3D modeling of drop morphology through constricted passages by using the scaling non dimensional parameters mentioned in the paper will enhance the understanding of the problem. The vast application of flow through porous structure, blood flow, mixing can be further explored.

References

1. S. Cobos, M. S. Carvalho, and V. Alvarado, "Flow of oil–water emulsions through a constricted capillary," *Int. J. Multiph. Flow* 35, 507–515 (2009).
2. W. L. Olbricht, "Pore-scale prototypes of multiphase flow in porous media," *Annual Review of Fluid Mechanics* 28(1), 187-213 (1996).
3. V. Joekar-Niasar, and S. M. Hassanzadeh, "Analysis of fundamentals of two-phase flow in porous media using dynamic pore-network models: a review," *Crit. Rev. Environ. Sci. Technol.* 42 (18), 1895-1976 (2012).
4. V. R. Guillen, M. S. Carvalho, and V. Alvarado, "Pore scale and macroscopic displacement mechanisms in emulsion flooding," *Trans. Porous Media* 94, 197-206 (2012).
5. P. A. Gauglitz, C. M. St. Laurent, and C. J. Radke, "Experimental determination of gas-bubble break-up in a constricted cylindrical capillary," *Indust. Engng Chem. Res.* 27, 1282-1291 (1988).
6. P. A. Gauglitz, and C. J. Radke, "The dynamics of liquid film break-up in constricted cylindrical capillaries." *J. Colloid Interface Sci.* 134, 1440 (1990).
7. A. Nazir, R. Boom, and K. Schroën, "Droplet break-up mechanism in premix emulsification using packed beds," *Chem. Eng. Sci.* 92, 190-197 (2013).
8. M. I. H. Khan, M. U. H. Joardder, C. Kumar, and M. A. Karim, "Multiphase porous media modelling: A novel approach to predicting food processing performance," *Crit. Rev. Food. Sci. Nutr.* 58(4), 528-546 (2018).
9. B. Nath, A. P. Bidkar, V. Kumar, A. Dalal, M. K. Jolly, S.S. Ghosh, and G. Biswas, "Deciphering hydrodynamic and drug-resistant behaviors of metastatic EMT breast cancer cells moving in a constricted microcapillary," *J. Clin. Med.* 8,1194 (2019).
10. R. Seemann, M. Brinkmann, T. Pfohl, and S. Herminghaus, "Droplet based microfluidics," *Rep. Prog. Phys.* 75, 016601 (2012).
11. S.L. Anna, "Droplets and bubbles in microfluidic devices," *Annu. Rev. Fluid Mech* 48, 285-309 (2016).
12. L. Shang, Y. Cheng, and Y. Zhao, "Emerging droplet microfluidics," *Chem. Rev.* 117, 7964–8040 (2017).
13. H. Feng, T. Zheng, M. Li, J. Wu, H. Ji, J. Zhang, W. Zhao, and J. Guo, "Droplet-based microfluidics systems in biomedical applications," *Electrophoresis* 40, 1580-1590 (2019).
14. S. Köster, F. E. Angile, H. Duan, J. J. Agresti, A. Wintner, C. Schmitz, A. C. Rowat, C. A. Merten, D. Pisignano, A. D. Griffiths, and D. A. Weitz, "Drop-based microfluidic devices for encapsulation of single cells" *Lab Chip* 8(7), 1110-1115 (2008).
15. C.N. Baroud, F. Gallaire, and R. Dangla, "Dynamics of microfluidic droplets," *Lab Chip* 10(16), 2032-2045 (2010).
16. G. F. Christopher, and S. L. Anna, "Microfluidic methods for generating continuous droplet streams," *J. Phys. D: Appl. Phys.* 40, R319–R336 (2007).
17. T. Fu, and Y. Ma, "Bubble formation and break-up dynamics in microfluidic devices: a review," *Chem. Engng Sci.* 135, 343–372 (2015).
18. P. B. Umbanhowar, V. Prasad, and D. A. Weitz, "Monodisperse Emulsion Generation via Drop Break Off in a Coflowing Stream," *Langmuir* 16, 347-351 (2000).
19. A. S. Utada, A. Fernandez-Nieves, H. A. Stone, and D. A. Weitz, "Dripping to jetting transitions in coflowing liquid streams," *Phys. Rev. Lett.* 99, 094502 (2007).

20. P. Garstecki, M. J. Fuerstman, H. A. Stone, and G. M. Whitesides, "Formation of droplets and bubbles in a microfluidic T-junction - scaling and mechanism of break-up," *Lab Chip* 6(3), 437–446 (2006).
21. M. de Menech, P. Garstecki, F. Jousse, and H. A. Stone, "Transition from squeezing to dripping in a microfluidic T-shaped junction," *J. Fluid Mech.* 595, 141–161 (2008).
22. T. Ward, M. Faivre, M. Abkarian, and H. A. Stone, "Microfluidic flow focusing: drop size and scaling in pressure versus flow-rate-driven pumping," *Electrophoresis* 26(19), 3716-3724 (2005).
23. S.L. Anna, N. Bontoux, and H.A. Stone, "Formation of dispersions using "flow focusing" in microchannels," *Appl. Phys. Lett.* 82, 364-366 (2003).
24. H. A. Stone, A. D. Stroock, and A. Ajdari, "Engineering flows in small devices: microfluidics toward a lab-on-a-chip," *Annu. Rev. Fluid Mech.* 36, 381–411 (2004).
25. H. Brenner, and J. Happel Slow viscous flow past a sphere in a cylindrical tube. *Journal of Fluid Mechanics*, 4(2), 195-213 (1958).
26. F. Bretherton, "The motion of long bubbles in tubes," *Journal of Fluid Mechanics* 10(2), 166-188 (1961).
27. H. L. Goldsmith, and S. G. Mason, "The flow of suspensions through tubes, Part II. Single large bubbles," *J. Colloid Sci.* 18, 237 (1963).
28. G. Hetsroni, S. Haber, and E. Wacholder, "The flow fields in and around a droplet moving axially within a tube," *Journal of Fluid Mechanics* 41(4), 689-705 (1970).
29. H. Brenner, "Pressure drop due to the motion of neutrally buoyant particles in duct flows," *Journal of Fluid Mechanics* 43(4), 641-660 (1970).
30. W. A. Hyman, and R. Skalak, "Viscous flow of a suspension of liquid drops in a cylindrical tube," *Appl. Sci. Res.* 26, 27–52 (1972).
31. B. Ho, and L. Leal, "The creeping motion of liquid drops through a circular tube of comparable diameter," *Journal of Fluid Mechanics* 71(2), 361-383 (1975).
32. E. I. Shen, and K. S. Udell, "A Finite Element Study of Low Reynolds Number Two-Phase Flow in Cylindrical Tubes," *ASME. J. Appl. Mech.* June 52(2), 253–256 (1985).
33. M. J. Martinez, and K. S. Udell, "Boundary Integral Analysis of the Creeping Flow of Long Bubbles in Capillaries," *ASME. J. Appl. Mech.* 56(1), 211–217 (1989).
34. M. Martinez, and K. Udell, "Axisymmetric creeping motion of drops through circular tubes," *Journal of Fluid Mechanics* 210, 565-591 (1990).
35. W. L. Olbricht, and D. M. Kung, "The deformation and break-up of liquid drops in low Reynolds number flow through a capillary," *Physics of Fluids A: Fluid Dynamics* 4, 1347 (1992).
36. W. Olbricht, and L. Leal, "The creeping motion of immiscible drops through a converging/diverging tube," *Journal of Fluid Mechanics* 134, 329-355 (1983).
37. L. Yan, K. E. Thompson, and K. T. Valsaraj, "A numerical study on the coalescence of emulsion droplets in a constricted capillary tube," *Journal of Colloid and Interface Science* 298, 832–844 (2006).
38. A. Z. Zinchenko, and R. H. Davis, "Motion of Deformable Drops Through Porous Media," *Annual Review of Fluid Mechanics* 49, 71-90 (2016).
39. T. Tsai, and M. Miksis, "Dynamics of a drop in a constricted capillary tube," *Journal of Fluid Mechanics* 274, 197-217 (1994).
40. C.-H. Chen, B. Hallmark, and J. F. Davidson, "The motion and shape of a bubble in highly viscous liquid flowing through an orifice," *Chemical Engineering Science* 206, 224-234(2019).
41. L. Cunha, I. R. Siqueira, E. L. Albuquerque, and T. F. Oliveira, "Flow of emulsion drops through a constricted microcapillary channel," *International Journal of Multiphase Flow* 103, 141-150 (2018).
42. J. T. Cabral, and S. D. Hudson, "Microfluidic approach for rapid multicomponent interfacial tensiometry," *Lab Chip* 6, 427-436 (2006).
43. J. M. Kohler, Th. Henkel, A. Grodrian, Th. Kirner, M. Roth, K. Martin, and J. Metze, "Digital reaction technology by micro segmented flow—components, concepts and applications," *Chem. Eng. J.* 101, 201–16 (2004).

44. A. Z. Zinchenko, and R. H. Davis, "A boundary-integral study of a drop squeezing through interparticle constrictions," *Journal of Fluid Mechanics* 564, 227-266 (2006).
45. R. E. Khayat, A. Luciani, L. A. Utracki, F. Godbille, and J. Picot, "Influence of shear and elongation on drop deformation in convergent-divergent flows," *International Journal of Multiphase Flow* 26, 17-44 (2000).
46. A. Leyrat-Maurin, and D. Barthes-Biesel, "Motion of a deformable capsule through a hyperbolic constriction," *Journal of Fluid Mechanics* 279, 135-163 (1994). doi:10.1017/S0022112094003848
47. J.F. Roca, and M.S. Carvalho, "Flow of a drop through a constricted microcapillary," *Computers & Fluids* 87, 50-56 (2013).
48. P. A. Gauglitz, C. M. St. Laurent, and C. J. Radke, "An Experimental Investigation of Gas-Bubble Break-up in Constricted Square Capillaries," *J. Pet. Technol.* 39, 1137 (1987). doi:10.2118/16183-PA
49. T. C. Ransohoff, P. A. Gauglitz, and C. J. Radke, "Snap-Off of Gas Bubbles in Smoothly Constricted Noncircular Capillaries," *AICHE Journal* 33, 753-765 (1987).
50. A. R. Kovscek, and C. J. Radke, "Gas bubble snap-off under pressure-driven flow in constricted noncircular capillaries," *Colloids and Surfaces A: Physicochemical and Engineering Aspects* 117, 55-76 (1996).
51. M. J. Martinez, and K. S. Udell, "Axisymmetric creeping motion of drops through a periodically constricted tube," *AIP Conference Proceedings* 197, 222 (1990).
52. T. Ratcliffe, A. Z. Zinchenko, and R. H. Davis, "Buoyancy-induced squeezing of a deformable drop through an axisymmetric ring constriction," *Physics of Fluids* 22, 082101 (2010).
53. A. Bordoloi, and E. Longmire, "Drop motion through a confining orifice," *Journal of Fluid Mechanics* 759, 520-545 (2014).
54. T. Patel, D. Patel, N. Thakkar, and Absar Lakdawala, "A numerical study on bubble dynamics in sinusoidal channels," *Physics of Fluids* 31, 052103 (2019).
55. M. Sauzade and T. Cubaud, "Bubbles in complex microgeometries at large capillary numbers," *Phys. Fluids* 26, 091109 (2014).
56. M. R. Bringer, C. J. Gerdts, H. Song, J. D. Tice, and R. F. Ismagilov, "Microfluidic systems for chemical kinetics that rely on chaotic mixing in droplets," *Phil. Trans. R. Soc. Lond. A* 362, 1087–104 (2004).
57. A. Liau, R. Karnik, A. Majumdar, and J.H.D. Cate, "Mixing crowded biological solutions in milliseconds," *Anal. Chem.* 77, 7618–25 (2005).
58. F. Sarrazin, L. Prat, N. Di Miceli, G. Cristobal, D. R. Link, and D. A. Weitz, "Mixing characterization inside microdroplets engineered on a microcoalescer," *Chem. Eng. Sci.* 62, 1042–8 (2007).
59. K. Y. Tung, C. C. Li, and J. T. Yang, "Mixing and hydrodynamic analysis of a droplet in a planar serpentine micromixer," *Microfluid. Nanofluid.* 7, 545–57 (2009).
60. Y. C. Tan, J. S. Fisher, A. I. Lee, V. Cristini and A. Phillip, "Design of microfluidic channel geometries for the control of droplet volume, chemical concentration, and sorting," *Lab Chip* 4, 292–8 (2004).
61. K. Liu, H. Ding, Y. Chen and X. Z. Zhao, "Droplet-based synthetic method using microflow focusing and droplet fusion," *Microfluid. Nanofluid.* 3, 239–43 (2007).
62. N. Bremond, A. R. Thiam, and J. Bibette, "Decompressing emulsion droplets favors coalescence," *Phys. Rev. Lett.* 100, 024501 (2008).
63. A. Lai, N. Bremond, and H. A. Stone, "Separation-driven coalescence of droplets: an analytical criterion for the approach to contact," *J. Fluid Mech.* 632, 97–107 (2009).
64. C. X. Zhao, and A. P. J. Middelberg, "Two-phase microfluidic flows," *Chem Eng Sci* 66(7), 1394–1411 (2011).